ELSEVIER

Dynamics of Atmospheres and Oceans
36 (2002) 3–21

dynamics of atmospheres and oceans

www.elsevier.com/locate/dynatmoce

On the horizontal density ratio in the upper ocean

Daniel L. Rudnick*, Joseph P. Martin

Scripps Institution of Oceanography, University of California, San Diego, Mail Code 0213, La Jolla, CA 92093-0213, USA

Received 31 July 2000; received in revised form 26 February 2001; accepted 26 February 2001

Abstract

The horizontal density ratio in the upper ocean is examined using SeaSoar data collected over the last 15 years in the Pacific, Atlantic, and Indian Oceans. The horizontal density ratio R is defined to be the ratio of the relative effect of temperature and salinity on density. A front with a horizontal density ratio of 1 is said to be compensated since temperature and salinity gradients compensate in their effect on density. The statistics of density ratio are examined through calculation of conditional probability density functions. Case studies from each of the oceans elucidate processes affecting the density ratio. Global distributions of density ratio are calculated as functions of mixed-layer depth, distance below the mixed layer, and magnitude of thermohaline variability. Compensation is found in all oceans, on 3–4 km horizontal scales, when the mixed layer is deep and significant thermohaline variability exists. The tendency for compensation is stronger as mixed-layer depth increases. Conversely, compensation is not typical in shallow mixed layers, or when thermohaline variability is weak. The thermocline density ratio is found to be 2, in agreement with previous observational studies, and consistent with the process of salt fingering. The transition from $R = 1$ in the mixed layer to $R = 2$ in the thermocline is sharp when the mixed layer is deep. The ubiquity of compensation in the mixed layer is consistent with recent theory that suggests horizontal eddy diffusivity is a growing function of density gradient.

Keywords: Upper ocean; Fronts; Mixed layer; Density ratio

1. Introduction

Fronts in the mixed layer are often observed to be warm and salty on one side and cool and fresh on the other such that the density contrast across the front is small. This phenomenon, termed compensation because temperature and salinity compensate in their effects on density, has been known for some time for certain fronts at scales of a few tens

* Corresponding author.
E-mail address: drudnick@ucsd.edu (D.L. Rudnick).

0377-0265/02/$ – see front matter
PII: S0377-0265(02)00022-2

to one hundred kilometers (Roden, 1975; Roden, 1984). More recently, compensation has been shown to exist at horizontal scales as small as 10 m (Rudnick and Ferrari, 1999; Ferrari and Rudnick, 2000). The purpose of this paper is to examine the tendency for compensation in the world's oceans.

A useful measure of the relative effect of temperature and salinity on density is the density ratio, defined as the change in density due to temperature divided by the change in density due to salinity. These changes are calculated by differencing measurements over a spatial interval. The density ratio has been extensively used to characterize thermohaline structure from vertical profiles, in which case spatial differencing is done in the vertical. Here the focus is on horizontal spatial differences. A compensated thermohaline front has a density ratio equal to 1. A front where the effect of temperature on density is opposed to but twice that of salinity has a density ratio of 2. A quantification of the horizontal density ratio in the mixed layer and seasonal thermocline of the global ocean is a goal here.

The existence of compensation in the mixed layer is consistent with density gradient driven horizontal mixing as proposed by Young (1994) and Ferrari and Young (1997). Consider a vertically mixed layer with an initially random distribution of temperature and salinity. Temperature and salinity gradients will compensate in their effect on density in some regions, while in others density gradients will exist. Density gradients will tend to slump due to gravity, creating sloping isopycnals (Fig. 1). Continued vertical mixing results in weakened horizontal density gradients. This process is essentially shear dispersion (Taylor, 1953) where the shear is due to slumping density gradients, and the mixing is caused by any of the processes that make the mixed layer vertically uniform. Temperature–salinity gradients that are compensated do not slump and therefore do not experience shear dispersion. The net effect is that density gradients diffuse while compensated gradients persist.

The Rossby radius of deformation for the mixed layer may be defined as $\sqrt{gH\delta\rho/\rho}/f$, where g is gravitational acceleration, H the thickness of the mixed layer, $\delta\rho$ the density difference across the mixed-layer base, ρ density, and f the inertial frequency. For a typical mixed layer at latitude 30°, H is 100 m, $\delta\rho$ 0.3 kg m^{-3}, g 9.8 m s^{-2}, and ρ 1025 kg m^{-3}, so the Rossby radius would be 7 km. The slumping and mixing model discussed is relevant

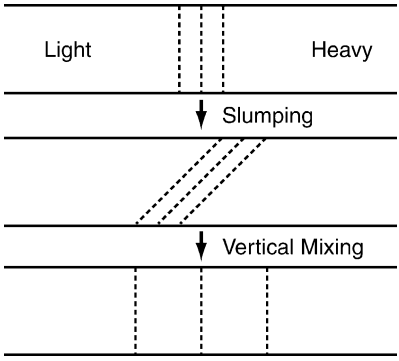

Fig. 1. The process of slumping and mixing is shown schematically. Consider a horizontal density gradient in a vertically mixed layer (top panel). The density gradient slumps due to gravity (middle panel). Vertical mixing results in a weakened density gradient (bottom panel). Thus, slumping and vertical mixing cause horizontal diffusion.

primarily for scales smaller than the Rossby radius of deformation, demonstrated to be of order 10 km. At larger scales, slumping can occur, as due to baroclinic or symmetric instability, but density gradients can persist in geostrophic balance. The phenomenon of compensation should thus be most prominent at scales smaller than about 10 km.

Mid-latitude thermocline waters are often found to have a density ratio equal to 2 on vertical scales of roughly 10–100 m (Schmitt, 1981). This phenomenon is believed to be caused by salt fingering (Schmitt, 1994). Salt fingers, a result of the very different molecular diffusivities of heat and salt, transport more salt than heat. Salt finger convection is a function of density ratio (where the temperature and salinity differences are taken over a vertical interval), strong when the density ratio is near 1 and weakening as the density ratio approaches 2. Thus, salt fingers increase the density ratio to a value of 2.

In this paper, SeaSoar data from the Pacific, Atlantic, and Indian Oceans are used to calculate the density ratio in the upper ocean. SeaSoar is a towed instrument that cycles from the surface to depths greater than 300 m. In typical use, SeaSoar completes a cycle once every 3–4 km at a tow speed of 8 knots. The historical SeaSoar database accumulated over the past 15 years provides a comprehensive view of the ocean's small-scale horizontal variability. This investigation is based on that data set.

The methods used to calculate the horizontal density ratio and its statistics are described in Section 2. Selected results from the North Pacific, North Atlantic, and Indian Oceans are described in detail in Sections 3–5. The entire data set is used to compute global statistics of the horizontal density ratio in Section 6. Finally, conclusions and a discussion are offered in Section 7.

2. Methods

The historical SeaSoar database is used in all of the following calculations. The data come from 11 cruises (Table 1), with several deployments per cruise. The cumulative length of all deployments (3.8×10^4 km) is nearly equal to the earth's circumference. The data are all from the mid-latitude open ocean. Relevant aspects of the data collection and processing are discussed below.

Table 1
A summary of the data used

Cruise name	Ocean	Latitude, longitude range	Dates (month (year))	Distance towed (km)
Spice	North Pacific	25–35°N, 122–140°W	1–2 (1997)	2647
FASINEX	North Atlantic	27–29°N, 70–71°W	4 (1986)	1223
Subduction 1	North Atlantic	29–34°N, 21–24°W	5–6 (1991)	2695
Subduction 2	North Atlantic	34–37°N, 20–25°W	3 (1992)	2523
Subduction 3	North Atlantic	20–33°N, 24–30°W	11–12 (1992)	3744
Subduction 4	North Atlantic	19–33°N, 21–38°W	5–6 (1993)	3691
Vivaldi	North Atlantic	39–48°N, 12–28°W	4–5 (1991)	5486
Arabian 1	Indian	14–18°N, 60–65°E	11–12 (1994)	3642
Arabian 2	Indian	14–18°N, 59–65°E	2 (1995)	4562
Arabian 3	Indian	14–18°N, 59–65°E	6–7 (1995)	4048
Arabian 4	Indian	15–18°N, 60–65°E	9–10 (1995)	3642

SeaSoars are equipped with CTDs to measure temperature, salinity, and pressure, allowing calculation of the horizontal density ratio. Calibration and processing of CTD data vary from cruise to cruise, as different kinds of CTDs are used in various configurations by a number of institutions. The data are typically collected at a frequency greater than once per second (24 Hz in the case of the Sea-Bird CTD). Many different procedures are used to minimize salinity spiking in the data (e.g. Lueck and Picklo, 1990). As an intermediate step, the data are often averaged to obtain a value every 1–3 s. Finally, the data are binned in the vertical with a resolution of 4–10 m, and either in time with a resolution of 12–15 min or in alongtrack distance with a resolution of 3–4 km. The temporal resolution is set by the typical period of the SeaSoar's sawtooth path. Since the tow speed is usually 4 m s^{-1}, the temporal and horizontal resolutions are roughly equivalent. The data are available to us in a variety of formats at different steps of the processing as discussed. In each case, we performed the additional processing required to create the binned data with horizontal resolution of 3–4 km.

The density ratio is defined as:

$$R \equiv \frac{\alpha \Delta\theta}{\beta \Delta S}, \tag{1}$$

where $\alpha = -\rho^{-1}(\partial\rho/\partial\theta)$ and $\beta = \rho^{-1}(\partial\rho/\partial S)$ are the expansion coefficients of temperature and salinity, $\Delta\theta$ and ΔS are horizontal differences of potential temperature and salinity, and ρ the density. The density ratio is calculated by differencing the binned data, and since the horizontal differencing is done over 3–4 km, the resolved wavelength is 6–8 km. We expect compensation to be most prevalent at scales less than the typical Rossby radius of deformation in the mixed layer (approximately 10 km). The horizontal scale of the observable density ratio is thus only marginally small enough to see compensation.

Because the density ratio is infinite when the salinity difference vanishes, we use the Turner angle:

$$\mathrm{Tu} = \arctan(R), \tag{2}$$

choosing the branch where $-\pi/2 \leq \mathrm{Tu} \leq \pi/2$. A compensated front with $R = 1$ thus has $\mathrm{Tu} = \pi/4$. An advantage of using the Turner angle is that temperature and salinity dominated regions occupy domains of equal size on the Tu axis. Further, the distribution of Tu is identical to that of $\mathrm{Tu}' = \arctan(R^{-1})$ with an offset of $\pi/2$. All statistics are calculated in terms of Tu. For convenience, results are discussed with reference to R, because its values are more familiar.

The distribution of density ratio in the upper ocean is examined using the probability density function (pdf) of Turner angle, $P(\mathrm{Tu})$. Practical estimation of the pdf requires definition of bins in Turner angle and calculation of the pdf as a histogram

$$P(\mathrm{Tu}) = \frac{n}{N\delta\mathrm{Tu}}, \tag{3}$$

where n is the number of data in a bin of size δTu centered at Tu, and a total of N data are used in the estimation. The pdf is thus normalized so that its integral with respect to Tu is 1. We use a bin size δTu of $\pi/50$ as a reasonable compromise between resolution and accuracy. An estimated pdf's root-mean-square (rms) error is approximately $\sqrt{P(\mathrm{Tu})/N\delta\mathrm{Tu}}$ (Bendat and Piersol, 1986). The rms error is thus larger for the mode of a pdf than for the tails.

Using (3), the error becomes $(\sqrt{n/N})/(\delta \mathrm{Tu}\sqrt{N})$. Because $n/N \leq 1$, an upper bound of the rms error of the pdf can be estimated given N and δTu. The smallest sample size used in calculating a pdf is 500, for which an upper bound of the rms error would be 0.71. Some of the pdfs have N >10,000 which implies an upper-bound rms error of <0.16. With these maximum errors, all the peaks in the estimated pdfs are significant. The pdfs of Tu are examined as functions of other observable variables, as, for example, depth z. Formally, the conditional pdf $P(\mathrm{Tu}|z)$ is used to make clear the normalization that the integral of $P(\mathrm{Tu}|z)$ with respect to Tu be 1 for all z (Papoulis, 1991).

The statistics of density ratio depend on whether the data are within or below the mixed layer, and vary as a function of mixed-layer depth. We define mixed-layer depth as the depth at which the potential density is 0.1 kg m^{-3} greater than the shallowest measurement (which is typically shallower than 10 m). Vertical interpolation of the potential density measurements is accomplished by a cubic spline.

3. North Pacific

Compensated mixed-layer fronts on scales of tens of kilometers and larger have been especially evident in the North Pacific (Roden, 1984). Results from the Spice experiment (Rudnick and Ferrari, 1999; Ferrari and Rudnick, 2000) have indicated that compensation is typical in the mixed layer on scales as small as 10 m. The tightness of the temperature–salinity relation in this previous work prompted the current study to verify that compensation on small scales is found in all mid-latitude oceans.

The Spice experiment was done to test ideas concerning the establishment of the T–S relation in the upper ocean. SeaSoar data were taken along a track extending from San Diego out to 140°W, and along 140°W between 25 and 35°N. The cruise was done in winter when vertical mixing was strong, making the data ideal for testing Young's theory of slumping and mixing. Along 140°W, mixed-layer depth varied from 100 to 150 m, near the annual maximum in this region of the ocean. A horizontal SeaSoar tow at 50 m in the mixed layer reveals compensation at all resolved scales (Fig. 2). Almost all fluctuations in temperature and salinity coincide to produce density compensation. The most striking feature is a sharp compensated front at 29.6°N, with a temperature jump of over 0.5 °C. This compensation can be seen graphically by plotting density and spice (Veronis, 1972; Munk, 1981). The horizontal difference in spice can be defined as:

$$\Delta\tau = \rho(\alpha\Delta\theta + \beta\Delta S). \tag{4}$$

Thus defined, spice is locally orthogonal to density in a θ–S plane scaled by the expansion coefficients. A global definition is necessary to study large-scale distributions of spice (Jackett and McDougall, 1985). A local definition is preferable here because the focus is small-scale variability, with all differences calculated at constant pressure. To generate a horizontal profile of spice, (4) is simply integrated horizontally. The difference in the variability of density and spice is obvious in Fig. 2. A few uncompensated features can be seen. An example is the strong salinity front just north of 29.4°N. Note that these data are from a horizontal tow. All subsequent data are derived from sawtooth tows that produce sections following the ship, with horizontal resolution of 3–4 km.

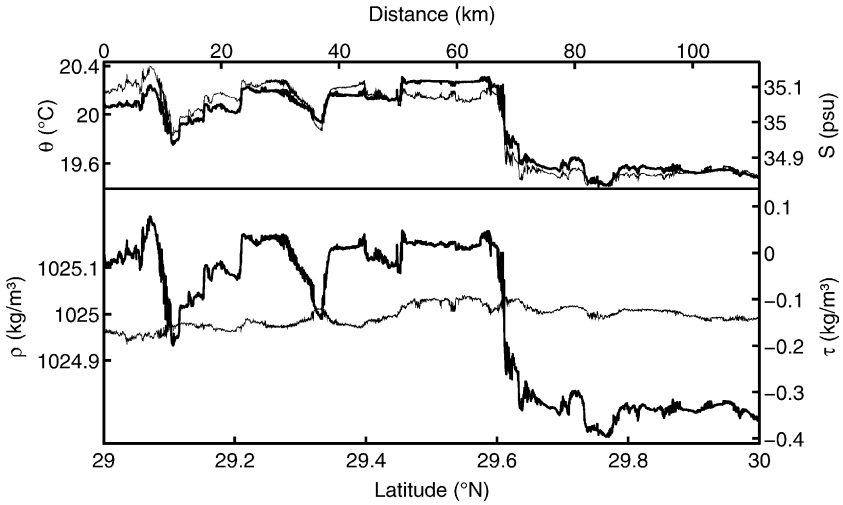

Fig. 2. Top panel: potential temperature (thin line, left axis) and salinity (thick line, right axis) from a horizontal SeaSoar tow at 50 m in the mixed layer of the North Pacific along 140°W. Vertical axes are scaled by the thermal and haline expansion coefficients so that fluctuations of temperature and salinity of equal size imply identical effects on density. Lower panel: density (thin line, left axis) and spice (thick line, right axis) for the same tow. Vertical axes are scaled so that fluctuations in density units are identical in the upper and lower panels. Latitude and distance are indicated on the lower and upper axes, respectively. Note the tendency toward compensation at all scales.

The compensation seen in Fig. 2 is typical of the mixed layer. The density ratio in the mixed layer is calculated from a section produced by a sawtooth tow along 140°W. The pdf of Turner angle (Fig. 3) in the mixed layer peaks near 1, showing the clear tendency for temperature and salinity gradients to compensate. The peak is skewed toward higher values of R, indicating that thermohaline gradients that are not compensated are more likely to be temperature dominated. One measure of a typical density ratio is the slope of the principal axis of the data as represented in the $\alpha\Delta\theta - \beta\Delta S$ plane (Rudnick and Ferrari, 1999). Using this measure, typical R would be 1.1, in reasonable agreement with the mode of the pdf.

Examining the conditional pdf of Turner angle as a function of depth reveals the different processes operating in the upper ocean (Fig. 4). The striking result is a rapid change in density ratio across the base of the mixed layer. The mixed-layer density ratio is typically 1, while the density ratio immediately beneath the mixed layer adopts a value of 2. Compensation is found at all depths in the mixed layer. The sub-mixed-layer density ratio of 2 is consistent with salt fingering. The sharp change in density ratio demonstrates the stark difference in processes acting above and below the mixed-layer base. The mixed layer is very strongly vertically mixed, an essential ingredient of the slumping and mixing mechanism. Beneath the mixed layer, turbulence is much weaker (Gregg, 1989; Ledwell et al., 1993), and double diffusion can operate to establish a density ratio of 2. The horizontal density ratio we calculate is quite analogous to a vertical density ratio, that is, where the differences in temperature and salinity are taken in the vertical. This occurs because isopycnals slope so that horizontal differences have a diapycnal component. In the thermocline, diapycnal thermohaline gradients

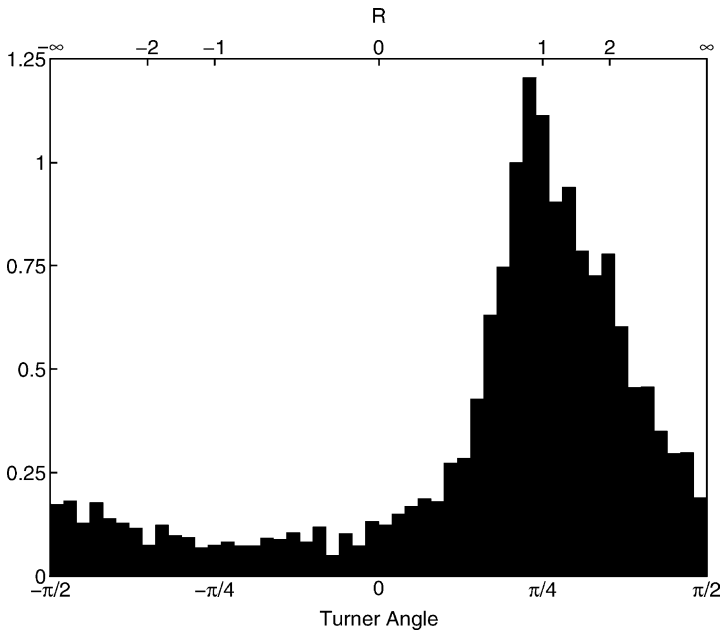

Fig. 3. Probability density function of mixed-layer Turner angle along 25–35°N, 140°W in the North Pacific. Turner angle and density ratio are indicated on the lower and upper axes, respectively. Note the mode at $R = 0.9$, where the pdf is 1.2. Total of 6992 data is used in the calculation so the pdf has an rms error of 0.05 at the mode.

are stronger than isopycnal thermohaline gradients, and horizontal and vertical density ratios are thus generally equivalent. The density ratio increases at 250 m and deeper as the salinity minimum of the North Pacific is encountered. Because this is a local extremum in salinity, while temperature is monotonic with depth, temperature dominates thermohaline gradients.

The positive skewness of the mixed-layer density ratio is possibly the result of entrainment of water with higher density ratio. If temperature and salinity gradients beneath the mixed layer are parallel, or equivalently, if the temperature–salinity relationship is linear:

$$\alpha T = R\beta S + C, \tag{5}$$

where C is a constant, then the density ratio R is conserved upon entrainment into the mixed layer. Consider initial conditions of no mixed layer, followed by entrainment down to a depth $z = -h(x, y)$. The temperature and salinity of the resulting mixed layer would be:

$$T_{\mathrm{m}} = \frac{1}{h}\int_{-h}^{0} T \,\mathrm{d}z, \qquad S_{\mathrm{m}} = \frac{1}{h}\int_{-h}^{0} S \,\mathrm{d}z. \tag{6}$$

Using (5 and 6), horizontal differences in mixed-layer temperature and salinity are related as follows:

$$\alpha \Delta T_{\mathrm{m}} = R\beta \Delta S_{\mathrm{m}}. \tag{7}$$

Assuming initial thermohaline gradients are inclined to the vertical, or mixed-layer depth is horizontally spatially variable, thermocline water retains its density ratio as it is entrained

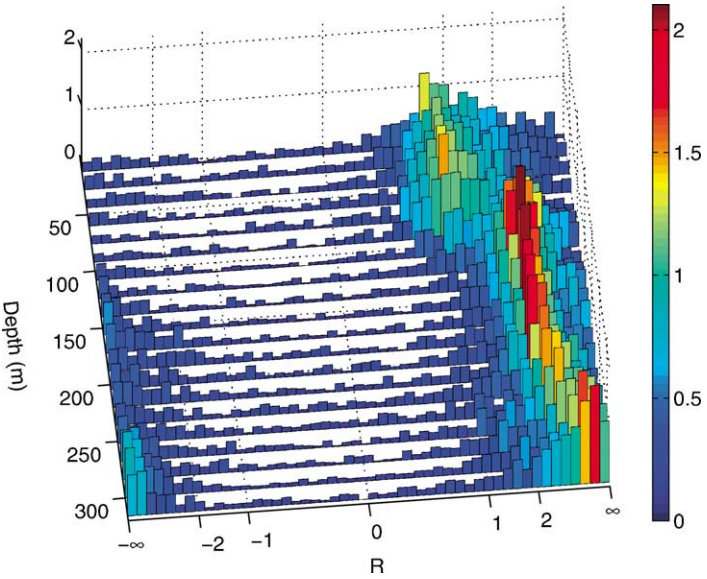

Fig. 4. Conditional probability density function of Turner angle Tu as a function of depth along 25–35°N, 140°W in the North Pacific. Each row of bars represents the conditional pdf for the given depth. Height, and color shading, of the bars indicate the pdf magnitude. The horizontal axis is labeled in units of density ratio R for convenience. Note the mode near 1 in the mixed layer and the rapid transition to a mode near 2 across the mixed-layer base. The density ratio increases below 250 m as the North Pacific salinity minimum is encountered. About 1000 data are used in the calculation for each depth and the pdf has maximum values near 2.0, so the pdf has a maximum rms error of 0.18.

into the mixed layer. The process of slumping and mixing will eventually cause compensation, but because entrained water typically has a density ratio of 2, the observed pdf is positively skewed (Fig. 3). Thus, positive skewness in the mixed layer is a reflection of thermohaline processes beneath the mixed layer.

Some conditions exist where thermocline water does not conserve its density ratio upon entrainment into the mixed layer. A trivial example is when initial thermocline gradients are exactly vertical and mixed-layer depth is horizontally uniform. Horizontal thermohaline gradients in the mixed layer would then be 0, and the density ratio would be undefined. If the thermocline temperature–salinity relationship is neither tight nor linear, contrary to (5), density ratio is not conserved after entrainment. In this hypothetical case, the thermocline density ratio is poorly defined, while observations indicate a tight and linear relationship with a density ratio of 2.

4. North Atlantic

The majority of the SeaSoar data used here are from the North Atlantic, the most observed of the world's oceans. Three experiments provide the data used here. The Subduction

experiment (Rudnick and Luyten, 1996; Rudnick, 1996; Joyce et al., 1998) was designed primarily to address the idea originally put forth by Iselin (1939) that late winter mixed-layer water is transported essentially unchanged along isopycnals to create thermohaline structure at depth. The Subduction experiment included a series of surveys of the Azores front at the subtropical gyre northern boundary, scattered mesoscale surveys within the gyre, and long sections. Among the first truly influential SeaSoar measurements are those from the Frontal Air-Sea Interaction Experiment (FASINEX, Pollard, 1986; Pollard and Regier, 1990; Pollard and Regier, 1992). The FASINEX data used here are derived from a survey in the subtropical frontal zone of the western North Atlantic. The Vivaldi experiment consisted of a large-scale survey north of the Azores (Pollard et al., 1996). These are the most northerly data analyzed, and exhibit the deepest mixed layers. Although, we do not discuss Vivaldi data explicitly, they are valuable in the global calculations.

A section across the Azores front (taken during the cruise Subduction 2) illustrates some common thermohaline features of the upper ocean (Fig. 5). The mixed layer is roughly 100 m deep, with a slanting density front between 35.6 and 35.8°N. Warm surface water caps the mixed layer north of the front. This restratification is understood because the survey was done in March at a time of increasing solar radiation. A temperature difference of 0.44 °C causes a density difference of 0.1 kg m^{-3}, at the average temperature and salinity of the section. The temperature contour interval of 0.4 °C is chosen to be close to this temperature difference, so that temperature and density contours can be compared to visualize the density

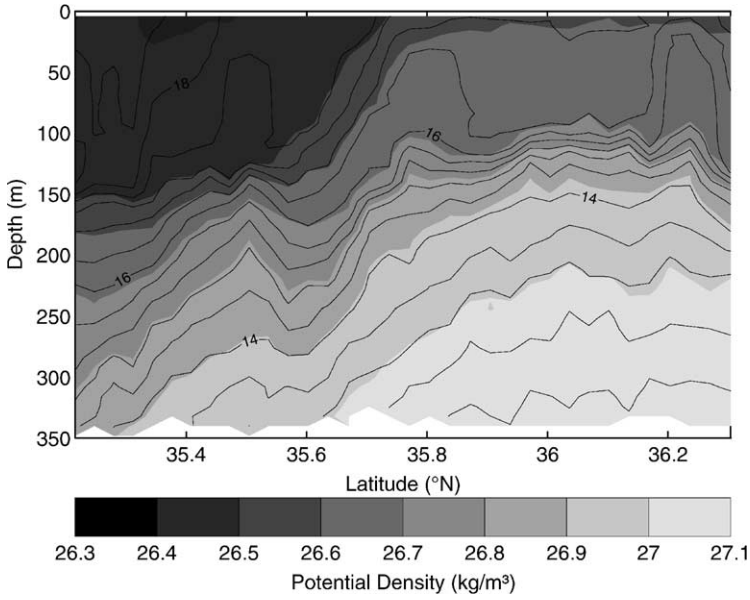

Fig. 5. A section of potential density and potential temperature across the Azores front in the North Atlantic along 24.25°W. Potential density is indicated by shading, with the contour interval 0.1 kg m^{-3}. Potential temperature is shown by lines, with a contour interval of 0.4 °C. The temperature contour interval is chosen to be close to the change in temperature (0.44 °C) that causes a 0.1 kg m^{-3} change in density. Compensated thermohaline features in the mixed layer, and $R = 2$ water in the thermocline, are evident.

ratio. Beneath the mixed layer, for example in the temperature range 14–16 °C south of the front, the density ratio is very nearly 2 as there are two temperature contours for every density contour. The mixed-layer density front also has a density ratio of approximately 2. Compensated temperature features are evident in the mixed layer on both sides of the front. An especially strong feature can be seen at the north end of the section.

Compensated thermohaline structure exists in consecutive sections taken along the front (Rudnick and Luyten, 1996). Thus, the compensated structure is in the form of streamers stretched out along the front by the straining geostrophic frontal flow. We have found that compensated streamers are typical features of frontal regions. The density ratio averaged over an area surrounding the front tends to be near 1 because most of the thermohaline structure (weighted by area) is compensated, while the front itself occupies a small area.

The visual inferences of density ratio from the section are representative of the complete frontal survey (Fig. 6). The density ratio is typically 1 in the mixed layer. Above 50 m, the distribution of density ratio broadens because of increasing stratification near surface. The density ratio increases abruptly to 2 across the base of the mixed layer near 100 m. The *T*–*S* relationships are strikingly similar in these data and those in the North Pacific, implying that the processes causing these relationships are the same in both oceans.

However, a mixed-layer density ratio of 1 is not always found. A counterexample is given by the FASINEX observations of the subtropical front in the western North Atlantic. The observations are from April, when the mixed layer is moderately deep at over 80 m. Salinity variability in the FASINEX data is so small as to be negligible relative to temperature

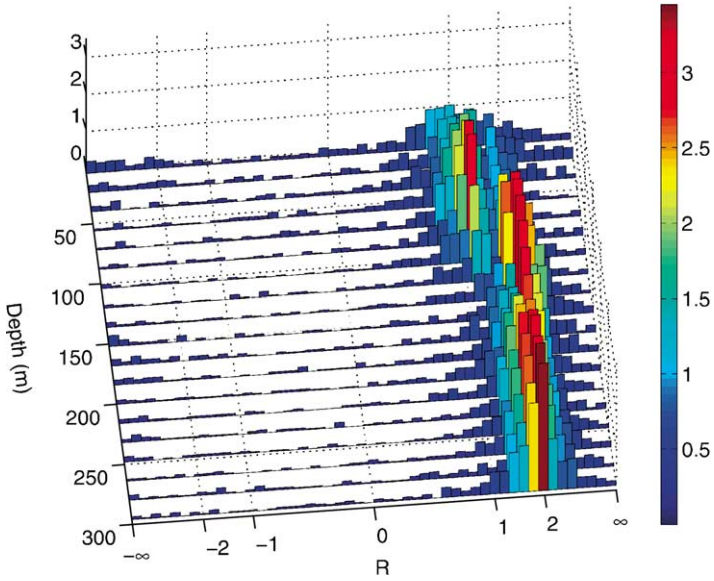

Fig. 6. Conditional probability density function of Turner angle with respect to depth for a survey of the Azores front in the North Atlantic. The density ratio changes abruptly from 1 in the mixed layer to 2 beneath. The near surface density ratio is poorly defined because of the onset of seasonal solar heating in March. About 600 data are used at each depth and the pdf has maximum values near 3.4, so the pdf has a maximum rms error of 0.30.

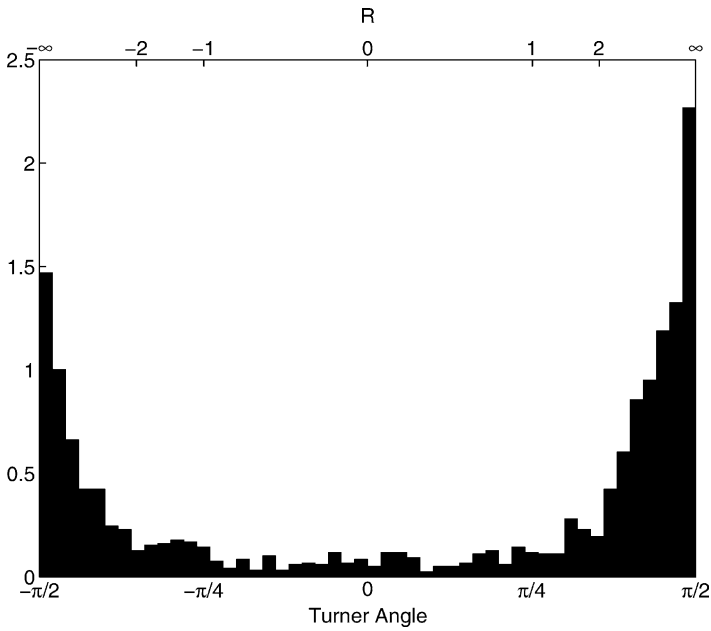

Fig. 7. Probability density function of mixed-layer Turner angle from a survey of the subtropical front in the western North Atlantic (FASINEX). The density ratio is large because so little salinity variability exists. Total of 1873 data is used and the maximum value of the pdf is 2.3, so the pdf has an rms error of 0.14.

variability. The result is a mixed-layer density ratio that is quite large (Fig. 7). For reference, the principal axis estimate of the density ratio is 23.6. The existence of some pre-existing salinity structure is necessary for compensation to develop through the slumping and mixing mechanism. One mechanism to create thermohaline structure is the stirring of large-scale gradients. The FASINEX region is characterized by weak large-scale salinity gradients, and therefore slight small-scale salinity variability. The FASINEX data demonstrate that not all regions of the ocean have compensated structure. These observations are consistent with theoretical results of Ferrari and Young (1997), which proves pre-existing variability in both temperature and salinity is required for compensation to develop. A second major class of examples when compensation is not found occurs when vertical mixing is weak. During times of stratification, as in summer, density ratio is poorly defined in that no sharp mode is found in the pdf. The shallowest depths of the Subduction frontal region (Figs. 5 and 6) offer one example. Taken as a whole, observations of noncompensation in the mixed layer indicate that necessary conditions for compensation are the existence of both temperature and salinity structure, and strong vertical mixing.

5. Indian

The thermohaline structure of the North Indian Ocean is intimately connected with the monsoon. In contrast to other mid-latitude locations, the Arabian Sea has two periods of

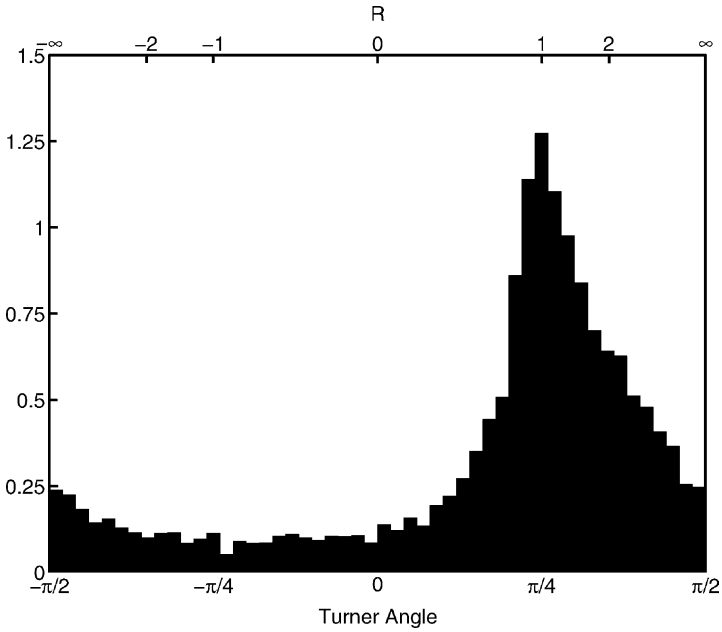

Fig. 8. Probability density function of mixed-layer Turner angle from the Arabian Sea in February. This is the time of the deepest mixed layers near the end of the NE monsoon when the atmosphere cools the ocean. The mode is 1.0, and the peak is skewed positively. Total of 9664 data is used and the maximum value of the pdf is 1.3, so the pdf has a maximum rms error of 0.05.

deep mixed layers each year. The winter NE monsoon produces the deepest mixed layers as the winds advect cool air southward from Asia (Rudnick et al., 1997). Wind mixing and thermal convection both act to deepen the mixed layer, as they do in all mid-latitude oceans in winter. The summer SW monsoon causes the mixed layer to deepen through wind mixing. However, surface heating of the ocean is usually positive, opposing the wind-driven mixing. We use data taken during extensive SeaSoar observations of the Arabian Sea throughout 1 year from 1994–1995 (Lee et al., 2000).

The density ratio in the Arabian Sea mixed layer depends on the phase of the monsoon cycle. Mixed-layer thermohaline gradients are typically compensated when vertical mixing is strong. A pdf of Turner angle is used to display results from February, the time of year with the deepest mixed layer (Fig. 8). The peak near $R = 1$ is positively skewed, as in the North Pacific, likely reflecting the entrainment of thermocline water with $R > 1$. The principal axis estimate of R is 1.2, in reasonable agreement with the pdf's mode. One would expect to find density ratios different from 1 during times of weak vertical mixing. The intermonsoon period following the SW monsoon is characterized by light winds and strong surface heating, and thus weak vertical mixing. The density ratio at this time is poorly defined, but >1 as temperature variability dominates salinity variability (Fig. 9). The mode approaches infinity, but the principal axis estimate of R is 2.1. The disagreement between

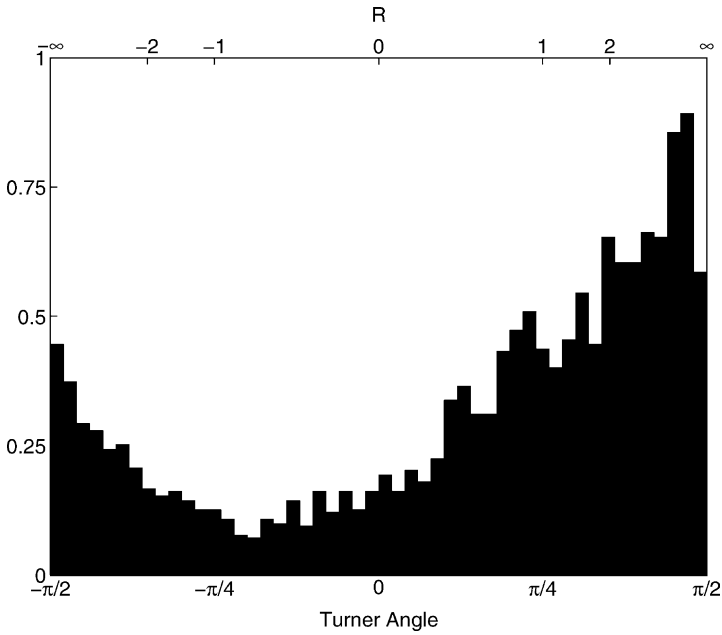

Fig. 9. Probability density function of mixed-layer Turner angle from the Arabian Sea in September/October. This is a time of weak winds and strong surface heating when vertical mixing is weak. The density ratio is greater than 1 as temperature variability dominates the shallow mixed layer. Total of 3481 data is used and the maximum value of the pdf is 0.9, so the pdf has a maximum rms error of 0.06.

the two measures of R occurs because the peak in the pdf is comparatively small, and R takes on a wide range of values.

Atmospheric forcing of the Arabian Sea is very different from the forcing of mid-latitudes of the Pacific and Atlantic. Arabian Sea atmospheric forcing is dominated by the biannual monsoonal cycle, while the mid-latitude Pacific and Atlantic have a dominant annual cycle and intense storms. In all these oceans, mixed-layer density compensation can be found when vertical mixing is strong.

6. Global

In the following, we address issues of global thermohaline behavior by combining all the data and examining conditional statistics. An important goal is to quantify the specific conditions under which compensation is typical in the mixed layer of the global ocean. The individual cases as discussed suggest that strong vertical mixing is crucial. The case studies also suggest that sub-mixed layer water typically has a density ratio of 2, in agreement with previous studies of central gyre waters (Schmitt, 1981). We examine the density ratio as a function of distance below the mixed layer to address the “twoness” of the thermocline.

Finally, we investigate if compensation depends upon the magnitude of the thermohaline gradients present in the mixed layer.

Strong vertical mixing is a required condition for density compensation in the mixed layer. We do not have measures of turbulence in the mixed layer, so we use mixed-layer depth as a surrogate measure of mixing strength: mixed layers become deep when vertical mixing is strong. The conditional pdf of mixed-layer Turner angle is calculated as a function of mixed-layer depth for the global data set (Fig. 10). At moderate mixed-layer depths between 25 and 75 m, the density ratio is poorly defined. For deep mixed layers greater than 75 m, a density ratio near 1 is typical. As mixed-layer depths increase, the peak in the pdf sharpens and the density ratio is even better defined. There is some tendency for the mode to be slightly greater than 1, and for the peak to be slightly skewed positively. At the smallest mixed-layer depths, temperature dominates density variability, and the peak in density ratio is large. However, we have relatively few data at the smallest mixed layer depths simply because the mixed layers are shallow. In all but the shallowest mixed-layer depth bin, there are more than 900 observations, so the peak in density ratio is likely robust.

The density ratio beneath the mixed layer has been known for some time to be close to 2 in the subtropical gyres of the world's oceans. Less clear is the transition from compensation in the mixed layer to $R = 2$ in the thermocline. In cases when vertical mixing is strong (that is, the mixed layer is deep) the density ratio transition from 1 to 2 is quite sharp (Figs. 4, 6). The transition tends to be less sharp when the mixed layer is shallow. The conditional pdf of Turner angle as a function of distance below the mixed layer helps to understand the depth dependence of thermocline R (Fig. 11). The mode in density ratio is slightly less than 2 deeper than 50 m below the mixed layer, consistent with previous results (Schmitt, 1981). Closer to the mixed-layer base, the density ratio may take a wide range of values. The region just below the mixed layer is characterized by strong vertical shears, particularly at the inertial frequency, which affect the density ratio as spice variability is differentially advected (Schmitt, 1990).

A relevant question is whether compensation is dependent on the magnitude of thermohaline variability in the mixed layer. This question is addressed by calculating the conditional pdf of Turner angle as a function of the magnitude of the thermohaline difference, defined as $\sqrt{(\alpha\Delta\theta)^2 + (\beta\Delta S)^2}$. To understand this definition, consider two fronts each of which have equal temperature and salinity gradients. Suppose one front has warm, fresh water on one side and cool, salty water on the other, and the second front separates warm, salty water from cool, fresh water. Thus, the first front is a pure density front, with no spice contrast, while the second front is purely spicy, with no density contrast. Each of these fronts would have the same thermohaline difference as defined.

A density ratio of 1 is typical at all except the smallest values of thermohaline difference (Fig. 12). The peak near $R = 1$ sharpens as thermohaline differences increase. For thermohaline differences of about 0.01 kg m^{-3} or less the distribution of density ratio broadens, and compensation is not as typical. In summary, the process of slumping and mixing is dominant when thermohaline gradients are strong. Other processes, such as mixing independent of density gradients, are relatively more important for small thermohaline differences.

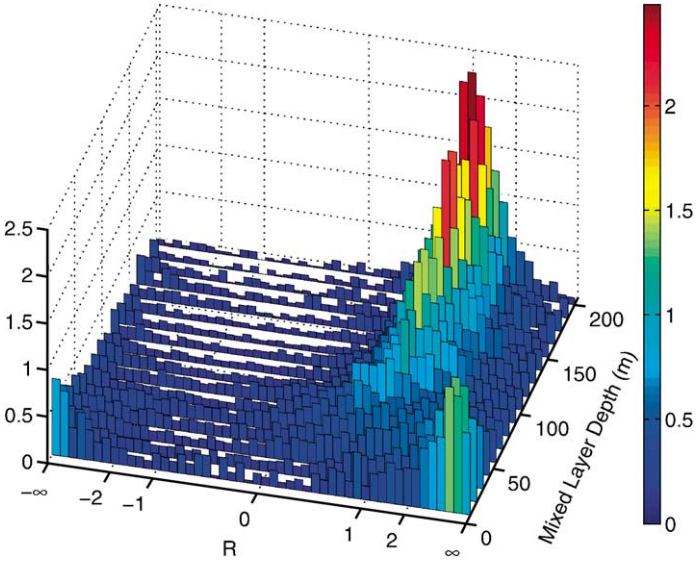

Fig. 10. Conditional probability density function of mixed-layer Turner angle as a function of mixed-layer depth from the global data set. The density ratio is typically 1 for mixed layers deeper than 75 m. The number of data at each mixed-layer depth is in the range 500–9000. The pdf has a maximum rms error approaching 0.2 for the shallowest and deepest mixed layers, where there are the fewest data. The best accuracy is for mixed-layer depths 50–100 m where maximum rms errors are 0.03–0.05.

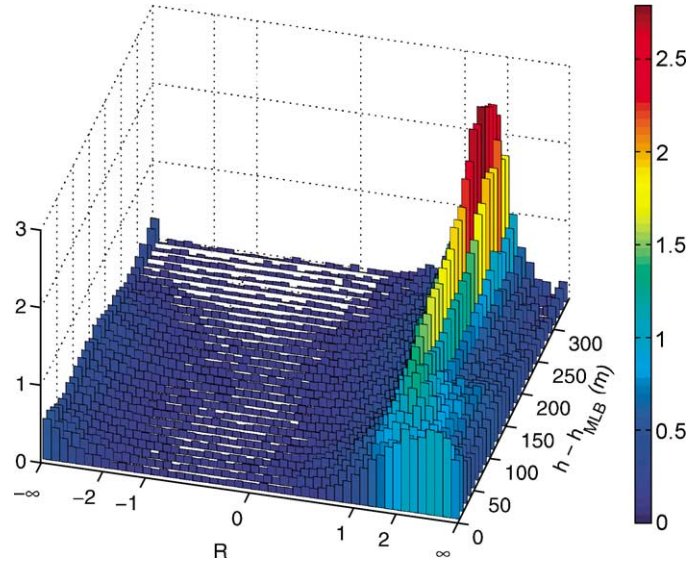

Fig. 11. Conditional probability density function of Turner angle as a function of distance below the mixed-layer base from the global data set. The density ratio is typically near 2 greater than 50 m beneath the mixed layer. The pdfs are calculated with 2000–16,000 data, and maximum rms errors are 0.03–0.14. Distances less than about 250 m below the mixed layer have the best accuracy, with maximum rms errors less than 0.05.

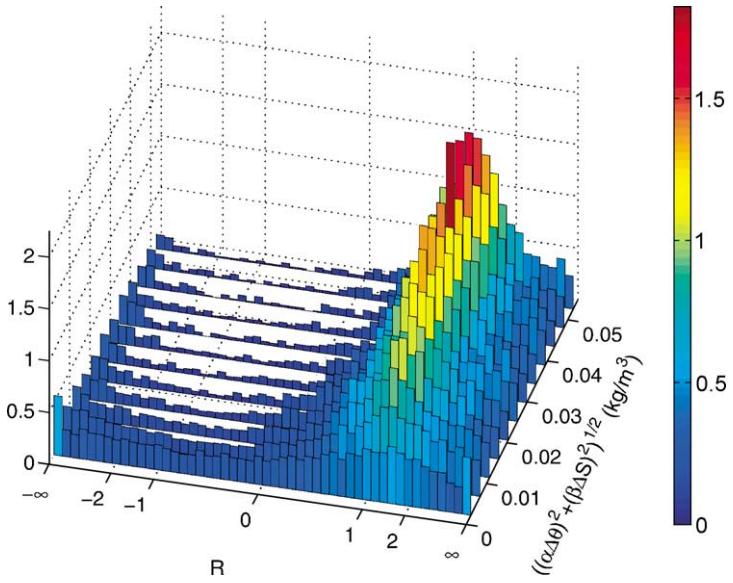

Fig. 12. Conditional probability density function of Turner angle as a function of the magnitude of thermohaline difference $\sqrt{(\alpha\Delta\theta)^2 + (\beta\Delta S)^2}$ from the global data set. The density ratio is near 1 for thermohaline differences larger than about 0.01 kg m^{-3}. The pdfs are calculated with 1000–14,000 data, and maximum rms errors are 0.03–0.15. The best accuracy is for small thermohaline differences.

7. Discussion and conclusion

Mixed-layer density compensation is ubiquitous in the global ocean when vertical mixing is strong. This conclusion is supported by individual observations in the Pacific, Atlantic, and Indian Oceans, and by examination of global SeaSoar data. That compensation is typical when the mixed layer exceeds about 75 m (Fig. 10) is convincing evidence that vertical mixing is crucial. A second rather trivial requirement for the presence of compensation is that variability exists in both temperature and salinity. The FASINEX data in the North Atlantic are an example with a moderately deep mixed layer, but negligible salinity variability and therefore, no compensation (Fig. 7). The two necessary conditions of strong vertical mixing and existing variability in temperature and salinity are consistent with theory (Ferrari and Young, 1997). Density compensation is typical whenever significant thermohaline gradients exist.

A clear, though hardly novel, result of our study is that the density ratio of the thermocline is typically 2. More significant is our finding of the depth below the mixed layer where the density ratio adopts the value 2. The transition from $R = 1$ to 2 can be quite sharp across the base of a deep, strongly mixed layer (Figs. 4 and 6). When the mixed layer is shallow and vertical mixing is relatively weak, the transition is less well defined. Averaging globally over mixed layers of many depths, the density ratio reaches 2 at least 50 m below the mixed-layer base. Our results are consistent with the usual interpretation of $R = 2$ being due to salt fingers (Schmitt, 1994).

The mechanisms establishing temperature–salinity relationships have long been a target of study for oceanographers. Stommel, in particular, revisited the problem many times, culminating in his last works (Stommel, 1993; Stommel and Young, 1993). Stommel observed that the large-scale horizontal mixed-layer density ratio is approximately 2 when differences are measured between the latitudes of 20 and 50°, a result supported in a more systematic study by Chen (1995). Stommel attempted a theoretical explanation of this observational fact using a two-box model in which salinity was forced stochastically, temperature was held at a fixed gradient, and mixing was dependent on density gradient. The recent theoretical work of Young and collaborators on slumping and mixing, the focused observational efforts of the Spice experiment, and the current study were all motivated by Stommel's study. Density compensation in the mixed layer is supported by extensive observations and a coherent theoretical explanation.

The process responsible for the observed large-scale mixed-layer density ratio of 2 remains undetermined. If density compensation is typical on scales smaller than 10 km, then the large-scale density ratio may be made of a series of density fronts separated by regions of compensated thermohaline variability. This hypothesis must be regarded as untested, but theoretical and observational studies may yet provide guidance. The results of our study should not be taken as evidence that horizontal density gradients do not exist in the winter mixed layer. Instead, density gradients are typically confined to frontal regions while most of the ocean has compensated thermohaline variability.

An implication for numerical modeling of the mixed layer is that horizontal mixing should be parameterized with a diffusivity that depends on density gradient. Existing observations cannot determine the functional form of the density gradient dependence. Young (1994) suggests the diffusivity should be proportional to the density gradient squared. Studies of length scales larger than the Rossby radius of deformation (∼10 km in the mixed layer) have proposed diffusivities proportional to the density gradient raised to powers of 1 (Visbeck et al., 1997; Haine and Marshall, 1998) to 3 (Pavan and Held, 1996). Experimental confirmation of any of these functional forms requires observing the decay of a horizontal density anomaly in a vertically mixed layer. Such an experiment might be reasonably attempted in the laboratory or the ocean.

Acknowledgements

We thank Bill Young and Raffaele Ferrari for inspiring discussions. The SeaSoar data used in this study are the result of hard work by too many individuals to mention. Some of those responsible are Jim Luyten, Terry Joyce, Raymond Pollard, Craig Lee, Ken Brink, and Lloyd Regier. The generous support of the Office of Naval Research (N00014-94-1-0251) and the National Science Foundation (OCE95-29752 and OCE98-19521) is gratefully acknowledged.

References

Bendat, J.S., Piersol, A.G., 1986. Random Data: Analysis and Measurement Procedures. Wiley, New York, 556 pp.
Chen, L.G., 1995. Mixed layer density ratio from the Levitus data. J. Phys. Oceanogr. 25 (4), 691–701.

Ferrari, R., Rudnick, D.L., 2000. Thermohaline variability in the upper ocean. J. Geophys. Res. 105 (C7), 16,857–16,883.

Ferrari, R., Young, W.R., 1997. On the development of thermohaline correlations as a result of nonlinear diffusive parameterizations. J. Mar. Res. 55, 1069–1101.

Gregg, M.C., 1989. Scaling turbulent dissipation in the thermocline. J. Geophys. Res. 94 (C7), 9686–9698.

Haine, T.W., Marshall, J., 1998. Gravitational, symmetric, and baroclinic instability of the ocean mixed layer. J. Phys. Oceanogr. 28, 634–658.

Iselin, C.O.D., 1939. The influence of vertical and lateral turbulence on the characteristics of waters at mid-depths. Trans. Am. Geophys. Union 20, 414–417.

Jackett, D.R., McDougall, T.J., 1985. An oceanographic variable for the characterization of intrusions and water masses. Deep-Sea Res. 32, 1195–1207.

Joyce, T.M., Luyten, J.R., Kubryakov, A., Bahr, F.B., Pallant, J.S., 1998. Meso- to large-scale structure of subducting water in the subtropical gyre of the eastern North Atlantic Ocean. J. Phys. Oceanogr. 28, 40–61.

Ledwell, J.R., Watson, A.J., Law, C.S., 1993. Evidence for slow mixing across the pycnocline from an open-ocean tracer-release experiment. Nature 364, 701–703.

Lee, C.M., Jones, B.H., Brink, K.H., Fischer, A.S., 2000. The upper-ocean response to monsoonal forcing in the Arabian Sea: seasonal and spatial variability. Deep-Sea Res. 47, 1177–1226.

Lueck, R.G., Picklo, J.J., 1990. Thermal inertia of conductivity cells: observations with a Sea-Bird cell. J. Atmos. Oceanic Technol. 7, 756–768.

Munk, W., 1981. Internal waves and small-scale processes. In: Warren, B.A., Wunsch, C. (Eds.), Evolution of Physical Oceanography. MIT Press, Cambridge, MA, pp. 264–291.

Papoulis, A., 1991. Probability, Random Variables, and Stochastic Processes. Communications and Signal Processing. McGraw-Hill, New York, 666 pp.

Pavan, V., Held, I.M., 1996. The diffusive approximation for eddy fluxes in baroclinically unstable jets. J. Atmos. Sci. 53 (9), 1262–1272.

Pollard, R., 1986. Frontal surveys with a towed profiling conductivity/temperature/depth measurement package (SeaSoar). Nature 323, 433–435.

Pollard, R.T., Griffiths, M.J., Cunningham, S.A., Read, J.F., Perez, F.F., Ríos, A.F., 1996. Vivaldi 1991—a study of the formation, circulation and ventilation of eastern North Atlantic central water. Prog. Oceanogr. 37, 167–192.

Pollard, R.T., Regier, L., 1990. Large variations in potential vorticity at small spatial scales in the upper ocean. Nature 348, 227–229.

Pollard, R.T., Regier, L.A., 1992. Vorticity and vertical circulation at an ocean front. J. Phys. Oceanogr. 22 (6), 609–625.

Roden, G.I., 1975. On North Pacific temperature, salinity, sound velocity and density fronts and their relation to the wind and energy flux fields. J. Phys. Oceanogr. 5, 557–571.

Roden, G.I., 1984. Mesoscale oceanic fronts of the North Pacific. Ann. Geophys. 2 (4), 399–410.

Rudnick, D.L., 1996. Intensive surveys of the Azores front. 2. Inferring the geostrophic and vertical velocity fields. J. Geophys. Res. 101 (C7), 16,291–16,303.

Rudnick, D.L., Ferrari, R., 1999. Compensation of horizontal temperature and salinity gradients in the ocean mixed layer. Science 283, 526–529.

Rudnick, D.L., Luyten, J.R., 1996. Intensive surveys of the Azores front. 1. Tracers and dynamics. J. Geophys. Res. 101 (C1), 923–939.

Rudnick, D.L., Weller, R.A., Eriksen, C.C., Dickey, T.D., Marra, J., Langdon, C., 1997. Moored instruments weather Arabian Sea monsoons, yield data, Eos. Trans. Am. Geophys. Union 78 (11), 117/120–121.

Schmitt, R.W., 1981. Form of the temperature-salinity relationship in the central water: evidence for double-diffusive mixing. J. Phys. Oceanogr. 11 (7), 1015–1026.

Schmitt, R.W., 1990. On the density ratio balance in the central water. J. Phys. Oceanogr. 20 (6), 900–906.

Schmitt, R.W., 1994. Double diffusion in oceanography. Ann. Rev. Fluid Mech. 26, 255–285.

Stommel, H.M., 1993. A conjectural mechanism for determining the thermohaline structure of the oceanic mixed layer. J. Phys. Oceanogr. 23 (1), 142–148.

Stommel, H.M., Young, W.R., 1993. The average *T*–*S* relation of a stochastically forced box model. J. Phys. Oceanogr. 23 (1), 151–158.

Taylor, G.I., 1953. Dispersion of soluble matter in solvent flowing slowly through a tube. Proc. Roy. Soc. London A 219, 186–203.

Veronis, G., 1972. On properties of seawater defined by temperature, salinity, and pressure. J. Mar. Res. 30 (2), 227–255.

Visbeck, M., Marshall, J., Haine, T., Spall, M., 1997. Specification of eddy transfer coefficients in coarse-resolution ocean circulation models. J. Phys. Oceanogr. 27, 381–402.

Young, W.R., 1994. The subinertial mixed layer approximation. J. Phys. Oceanogr. 24, 1812–1826.